ELSEVIER

Neuropsychologia 45 (2007) 476–483

NEUROPSYCHOLOGIA

www.elsevier.com/locate/neuropsychologia

Activity and effective connectivity of parietal and occipital cortical regions during haptic shape perception

Scott Peltier [b], Randall Stilla [a], Erica Mariola [a], Stephen LaConte [b], Xiaoping Hu [b], K. Sathian [a,*]

[a] *Department of Neurology, Emory University School of Medicine, Atlanta, GA, United States*
[b] *Coulter Department of Biomedical Engineering, Emory University School of Medicine and Georgia Institute of Technology, Atlanta, GA, United States*

Received 3 September 2005; received in revised form 12 January 2006; accepted 3 March 2006
Available online 17 April 2006

Abstract

It is now widely accepted that visual cortical areas are active during normal tactile perception, but the underlying mechanisms are still not clear. The goal of the present study was to use functional magnetic resonance imaging (fMRI) to investigate the activity and effective connectivity of parietal and occipital cortical areas during haptic shape perception, with a view to potentially clarifying the role of top-down and bottom-up inputs into visual areas. Subjects underwent fMRI scanning while engaging in discrimination of haptic shape or texture, and in separate runs, visual shape or texture. Accuracy did not differ significantly between tasks. Haptic shape-selective regions, identified on a contrast between the haptic shape and texture conditions in individual subjects, were found bilaterally in the postcentral sulcus (PCS), multiple parts of the intraparietal sulcus (IPS) and the lateral occipital complex (LOC). The IPS and LOC foci tended to be shape-selective in the visual modality as well. Structural equation modelling was used to study the effective connectivity among the haptic shape-selective regions in the left hemisphere, contralateral to the stimulated hand. All possible models were tested for their fit to the correlations among the observed time-courses of activity. Two equivalent models emerged as the winners. These models, which were quite similar, were characterized by both bottom-up paths from the PCS to parts of the IPS, and top-down paths from the LOC and parts of the IPS to the PCS. We conclude that interactions between unisensory and multisensory cortical areas involve bidirectional information flow.

Keywords: Multisensory; Visual; Tactile; Functional magnetic resonance imaging (fMRI); Structural equation modeling (SEM)

1. Introduction

Numerous studies by many groups have shown that human tactile perception evokes activity, not only in somatosensory cortical areas, but also in visual cortical areas. Our laboratory was the first to report this, on the basis of a functional imaging study (Sathian, Zangaladze, Hoffman, & Grafton, 1997) in which tactile discrimination of grating orientation activated a parieto-occipital cortical region (POC) that was previously reported to be active during visual discrimination of grating orientation (Sergent, Ohta, & MacDonald, 1992). Subsequently, we found that transcranial magnetic stimulation over POC disrupts tactile grating orientation discrimination (Zangaladze, Epstein, Grafton, & Sathian, 1999), thus establishing the importance of POC activity for tactile perception. Others have reported that perception of tactile motion recruits the MT complex, a visual motion-selective area (Blake, Sobel, & James, 2004; Hagen et al., 2002). Similarly, the lateral occipital complex (LOC), which was originally described as an object-selective region in the ventral visual pathway (Malach et al., 1995), is activated during tactile perception of two-dimensional patterns (Prather, Votaw, & Sathian, 2004; Stoesz et al., 2003) and haptic perception of three-dimensional objects (Amedi, Jacobson, Hendler, Malach, & Zohary, 2002; Amedi, Malach, Hendler, Peled, & Zohary, 2001; Reed, Shoham, & Halgren, 2004; Stoeckel et al., 2003; Zhang, Weisser, Stilla, Prather, & Sathian, 2004). Such observations indicate that areas generally considered visual are also recruited during tactile perception, in a task-specific manner

* Corresponding author at: Department of Neurology, Emory University School of Medicine, WMRB 6000, 101 Woodruff Circle, Atlanta, GA 30322, United States. Tel.: +1 404 727 1366; fax: +1 404 727 3157.
E-mail address: krish.sathian@emory.edu (K. Sathian).

0028-3932/$ – see front matter © 2006 Elsevier Ltd. All rights reserved.
doi:10.1016/j.neuropsychologia.2006.03.003

(Sathian, Prather, & Zhang, 2004). However, the mechanisms underlying such cross-modal recruitment remain uncertain. One possible mechanism is visual imagery, as we have suggested previously (Sathian et al., 1997; Sathian & Zangaladze, 2001; Stoesz et al., 2003; Zangaladze et al., 1999; Zhang et al., 2004). Another possibility is that both visual and tactile processing engage a common multisensory representation (Amedi et al., 2001; Amedi et al., 2002; James et al., 2002). The first possibility implies involvement of top-down connections into visual cortical areas (Mechelli et al., 2004), while the second might involve bottom-up tactile inputs. Examining the connectivity of the active areas could therefore help to distinguish between these possibilities.

Effective connectivity can be studied using structural equation modelling (SEM) of imaging data, which allows the statistical analysis of causal relationships by examining correlations between time-courses of activity in different regions and constructing models of their interaction (Büchel & Friston, 2001; McIntosh & Gonzalez-Lima, 1994). The parameters in such a model are the connection strengths (path weights) between different variables, which reflect the effective connectivity in the network. These parameters are estimated by minimizing the difference between the observed covariances and those implied by a given structural model. Recently, exploratory SEM of functional magnetic resonance imaging (fMRI) data was introduced (Zhuang, LaConte, Peltier, Zhang, & Hu, 2005). This approach tests and ranks all possible models for empirical fit to activation data, arriving at a model that best accounts for the observed fMRI activity. It can be viewed as a complement to other exploratory approaches employed in the fMRI literature, such as independent component analysis (Calhoun, Adali, Pearlson, & Pekar, 2001; McKeown et al., 1998) or clustering (Ngan & Hu, 1999). In this report, we investigate the activity and effective connectivity of haptic shape-selective regions in parietal and occipital cortex using fMRI and exploratory SEM.

2. Methods

2.1. Subjects

Six neurologically normal subjects (3 male, 3 female) took part in this study after giving informed consent. Their ages ranged from 19 to 24 years (mean, 22). All subjects were right-handed, as assessed by the high-validity subset of the Edinburgh handedness inventory (Raczkowski, Kalat, & Nebes, 1974). Subjects with a history of injury to the hands or their innervation were excluded, as were those with a history of dyslexia, which is associated with tactile impairments (Grant, Zangaladze, Thiagarajah, & Sathian, 1999; Sathian et al., 2003). All procedures were approved by the Institutional Review Board of Emory University.

2.2. Stimulation

Stimuli were sets of objects varying in three-dimensional shape, or sets of textures. Different sets of shapes and textures were used for haptic and visual presentations. The haptic shapes (HS) were meaningless objects with smooth, painted surfaces, measuring approximately the same (5 cm × 5 cm × 2.5 cm), but varying in shape and configuration. The haptic textures (HT) consisted of 4 cm × 4 cm × 0.3 cm cardboard substrates onto which textured fabric or upholstery was adhered. Thus, the shapes were all of identical texture and the textures were all of identical shape and size. An experimenter placed haptic stimuli in the subject's open hand. The stimuli were consistently presented in a fixed orientation, and subjects were instructed not to rotate or re-orient objects during exploration. Subjects were never allowed to see the haptic stimuli, and their eyes were closed during haptic exploration. During the corresponding visual conditions, subjects viewed photographs of either shapes or textures, displayed centrally on a black screen. The images used for visual presentations were scanned into a computer, grayscaled, and resized to 5° square using Adobe Photoshop. Visual shapes (VS) were photographs of objects of the same type as the haptic shapes. Photographs of common textures (Brodatz, 1966) were used to generate the visual texture (VT) stimuli.

2.3. MR scanning

MR scans were performed on a 3 Tesla Siemens Trio whole body scanner (Siemens Medical Solutions, Malvern, PA), using a standard quadrature headcoil. Functional images with blood oxygenation level-dependent (BOLD) contrast were acquired using a $T2^*$-weighted single-shot gradient-recalled echo-planar imaging (EPI) sequence. Axial slices of 5 mm thickness were acquired to provide full-brain coverage (25 slices in four subjects and 21 in the other two) with the following parameters: repetition time (TR) 2000 ms, echo time (TE) 30 ms, flip angle (FA) 90°, in-plane resolution 3.4 mm × 3.4 mm, in-plane matrix 64 × 64. High-resolution anatomic images were also acquired, using a 3D magnetization-prepared rapid acquisition gradient echo (MPRAGE) sequence (TR 2300 ms, TE 3.9 ms, inversion time 1100 ms, FA 8°) consisting of 176 sagittal slices of 1 mm thickness (in-plane resolution 1 mm × 1 mm, in-plane matrix 256 × 256).

The subject lay supine in the scanner with the right arm outstretched beside the body. When advanced to the scan position (head centered in the magnet bore), the subject's right hand was located at the flared magnet aperture, fully accessible and free to haptically explore objects. Foam padding under the body, wrapped around the right arm and under the right hand, was used to minimize movement and transfer of vibration from the gradient coils and ensure the subject's comfort. A mirror positioned above the subject's eyes provided unobstructed visualization of images projected on a screen at the rear magnet aperture. Head restraint straps and foam blocks were utilized to minimize head movement. Sound-attenuating headphones were used to muffle scanner noise and also served to convey verbal cues (see below). Separate haptic and visual stimulation runs were performed. A block design paradigm was used in which blocks with and without stimulation alternated. Non-stimulation (baseline) blocks began and ended each run. In each modality, shape and texture blocks were pseudo-randomly interleaved, with different sequences for each subject. Each type of stimulation block was repeated six times in a run.

In each haptic trial, an experimenter placed stimuli in the subject's right hand for 5 s, with a 1 s inter-stimulus interval. In the inter-stimulus intervals, the subject pressed one of two buttons on a fiberoptic response box, with the second or third digit of the left hand, to indicate whether the stimulus was identical to or different from the immediately preceding stimulus. The onset of baseline blocks was verbally cued with the word "rest". Immediately preceding each stimulation block, subjects were cued with the words "shape" or "texture" to instruct them which task would follow. The sequence and timing of object presentation were guided by pre-programmed instructions displayed to the experimenter on a computer screen using the Presentation software package, which also recorded responses. Subjects kept their eyes closed during the haptic runs.

Throughout the visual runs, subjects fixated on a cross in the center of a black screen. Visual stimuli were presented for 1 s per trial with a 1 s inter-stimulus interval. For both visual and haptic runs, baseline blocks lasted for 16–20 s (16 s in 2 subjects, 18 s in 1 subject and 20 s in 3 subjects). Visual stimulation blocks were of the same duration as the corresponding baseline blocks for each subject; haptic stimulation blocks were always 30 s long. Each subject took part in 2 haptic runs. The two subjects for whom visual stimulation block duration was 16 s participated in 3 visual runs; the remaining four subjects took part in 2 visual runs. Thus, there were 60 haptic trials per condition, while the number of visual trials per condition varied somewhat (144 trials for 2 subjects, 108 trials for 1 subject, and 120 trials for 3 subjects). This variation was because the number of visual trials was progressively increased over the course of the study, in order to increase the signal-to-noise ratio. Apart from these minor differences, the visual runs were similar to the haptic runs.

2.4. Image processing and analysis

Image processing and analysis was performed using BrainVoyager QX v1.1 (Brain Innovation, Maastricht, The Netherlands). Each subject's BOLD images were realigned to the first image of the series using a rigid-body transformation procedure. Functional 2D images were pre-processed utilizing trilinear interpolation for motion correction, sinc interpolation for slice scan time correction, and high-pass temporal filtering at 1 Hz to remove slow drifts in the data. Anatomic 3D images were processed, co-registered with the functional data, and transformed into Talairach space (Talairach & Tournoux, 1988). Since analysis was performed on an individual subject basis, the imaging data were not spatially smoothed. Statistical analysis in individual subjects used the general linear model (GLM) and a contrast of the shape and texture conditions to identify shape-selective regions, with correction for multiple comparisons ($q < 0.05$) by the false discovery rate (FDR) approach (Genovese, Lazar, & Nichols, 2002) implemented in BrainVoyager QX.

2.5. Effective connectivity analysis

Since our goal was to investigate the effective connectivity of haptic shape-selective areas, regions of interest (ROIs) in the parietal and occipital lobes were identified using the contrast HS–HT for each subject. As detailed in the Results section, five such bilateral ROIs were consistently active across subjects. Since the right hand was stimulated, the ROIs for connectivity analysis were taken from the left hemisphere, and were constrained not to exceed a cubic volume of 8 mm^3, centered on the peaks of the activations. For each subject, the signal intensities were averaged across voxels of each ROI to derive a signal time-course during all conditions of the two haptic runs. These values were then normalized by dividing each value by the mean value for the ROI per run. The normalized time-courses were then concatenated across all subjects and runs to form a single vector per ROI and the correlation matrix between ROI time-courses was computed.

Using the above five ROIs, all possible two-way interactions were considered, resulting in 20 possible paths between ROIs. This results in $2^{20} = 1{,}048{,}576$ possible structural interactions, which were automatically generated using custom software developed in Matlab (MathWorks, Natick, MA). The SEM software Lisrel 8.72 (Jöreskog and Sorbom, Scientific Software International Inc., Chicago, IL) was used to fit each structural interaction to the experimental data and estimate its statistical significance. The models were sorted by their fit indices, using the method of connectivity exploration developed by Zhuang et al. (2005). The method consists of three steps: (1) model estimation, (2) model evaluation, and (3) model ranking. The model estimation step is simply the fitting of each possible structural interaction (using Lisrel). Model evaluation is used to eliminate unacceptable models, based on path coefficients and model complexity. Specifically, models with t-values outside 95% confidence limits or with excessive parsimony goodness of fit indices (PGFI; we used an upper threshold of 0.1) were eliminated. Finally ranking is performed on all surviving models, first using the adjusted goodness of fit index (AGFI), which accounts for the number of degrees of freedom in the model, with values >0.9 being considered a good fit (Hu and Bentler, 1999); then secondly ranked by the largest standardized residual, which indicates the overall degree of discrepancy in fitting the hypothesized and observed covariance, with values approaching zero indicating a good fit. For the top-ranked models, we also used additional fit indices that were not used in the ranking process to verify goodness of fit (Kline, 1998): χ^2/d.f. = 0.009 [<2 being considered a good fit (Ullman, 1996)], and root mean square error of approximation (RMSEA) [<0.08 indicating a good fit (Hu & Bentler, 1999)].

3. Results

3.1. Behavioral

Average accuracy on all tasks was 90% correct or better. On each visual task, accuracy was $95 \pm 0.8\%$ correct (mean ± S.E.M.). Accuracy was $90 \pm 2.3\%$ correct for HS and $92 \pm 1.8\%$ correct for HT. A one-way analysis of variance showed that there was no significant effect of task on accuracy ($F = 0.69$; $p = 0.57$). Since performance did not differ significantly across conditions, it is reasonable to conclude that the tasks were balanced for difficulty.

3.2. Activations

We focus here on significant activations in parietal and occipital regions on the HS–HT contrast, that were found consistently in each of the six subjects. Five such regions were bilaterally active: one in the postcentral sulcus (PCS); three in the intraparietal sulcus (IPS), one anterior (aIPS), one posterior (pIPS) and one ventral (vIPS); and one in the LOC. Table 1 gives the Talairach coordinates of the peaks of these activations in each subject. Fig. 1 shows their locations in a representative subject, and Fig. 2 illustrates the time-course of the BOLD signal at

Table 1
Talairach coordinates of peaks of haptic shape-selective activations

	Left			Right		
	x	*y*	*z*	*x*	*y*	*z*
Subject 1						
PCS	−35	−28	64	47	−30	49
aIPS	−38	−47	49	**35**	**−54**	**49**
pIPS	−18	−71	49	25	−69	51
vIPS	**−25**	**−70**	**31**	31	−68	29
LOC	**−45**	**−56**	**−6**	**53**	**−58**	**−6**
Subject 2						
PCS	−37	−31	55	51	−20	49
aIPS	−32	−31	47	**28**	**−47**	**60**
pIPS	**−14**	**−59**	**48**	15	−65	53
vIPS	−20	−66	33	**33**	**−67**	**34**
LOC	**−46**	**−60**	**2**	**52**	**−55**	**−1**
Subject 3						
PCS	−39	−36	59	48	−31	53
aIPS	−40	−34	48	38	−47	54
pIPS	−18	−60	45	21	−66	53
vIPS	−26	−57	27	32	−60	27
LOC	−48	−54	2	51	−51	−7
Subject 4						
PCS	**−50**	**−34**	**42**	**57**	**−28**	**40**
aIPS	**−34**	**−46**	**46**	**39**	**−34**	**40**
pIPS	**−9**	**−78**	**41**	**13**	**−75**	**45**
vIPS	**−26**	**−77**	**26**	**32**	**−72**	**27**
LOC	**−50**	**−63**	**−9**	**43**	**−65**	**−12**
Subject 5						
PCS	−45	−34	47	53	−23	39
aIPS	**−37**	**−27**	**38**	**41**	**−31**	**37**
pIPS	**−22**	**−61**	**49**	**24**	**−60**	**43**
vIPS	**−26**	**−60**	**30**	**35**	**−58**	**22**
LOC	**−45**	**−57**	**−4**	**53**	**−58**	**−8**
Subject 6						
PCS	−32	−30	66	56	−22	43
aIPS	**−31**	**−38**	**50**	**43**	**−34**	**49**
pIPS	**−9**	**−61**	**57**	**28**	**−60**	**56**
vIPS	**−11**	**−84**	**35**	**26**	**−82**	**34**
LOC	**−43**	**−64**	**0**	**45**	**−55**	**2**

Bold type indicates regions that were also visually shape-selective. See text for details.

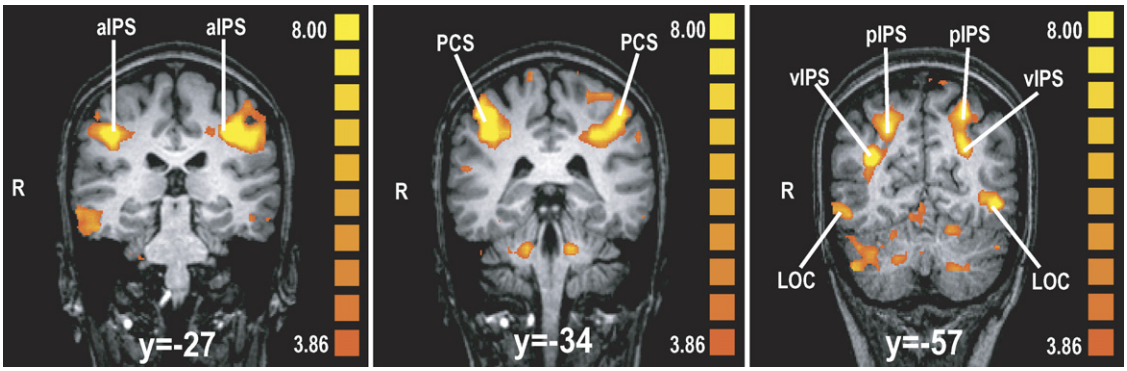

Fig. 1. Locations of parieto-occipital activations on HS–HT contrast in subject 5, displayed on coronal slices through this subject's anatomic image. Talairach y positions are given below each slice. See text for abbreviations.

each of these sites in the left hemisphere for the two stimulation conditions in each modality, in the same subject. The left column of Fig. 2 demonstrates that there was greater BOLD signal increase during the HS than the HT condition at each of these locations. Such haptic shape-selectivity was true of all subjects for both hemispheres. The right column reveals that visual shape-selectivity varied across sites.

In order to evaluate whether the haptic shape-selective regions also showed significant shape-selectivity in the visual modality, we performed a conjunction analysis across modalities, in individual subjects, i.e. (HS–HT) + (VS–VT). In Table 1, the coordinates of haptic shape-selective regions that were also visually shape-selective are indicated in bold type. Such bisensory regions were found in the LOC bilaterally and the right aIPS in 5 subjects; in the vIPS bilaterally and the left pIPS in 4; in the right pIPS and left aIPS in 3; and in the PCS bilaterally in only 1 subject.

3.3. *Effective connectivity analysis*

The top-ranked effective connectivity models are shown in Fig. 3. These two models were equivalent (fit the data equally well), with AGFI = 1.00, largest standardized residual = 0.0001, χ^2/d.f. = 0.009, and RMSEA = 0.0 (0.999 probability of a good fit). In addition, all path coefficients were significant. Table 2 displays the standardized path weights and *t* values for every path in these models. The standardized path weight corresponds to the change of activity in the target of the path for a unit change of activity at the source of that path. The sign of the path weight reflects the sign of the correlation between target and source of the path. The two models were similar in many respects (see Fig. 3 and Table 2). The chief differences were whether aIPS and pIPS project to vIPS (Model A) or LOC (Model B), and the reversal of the vIPS–LOC connection between the two models.

Table 2
Standardized path weights and *t* values for all paths in the two top-ranked models illustrated in Fig. 3

Path	Model A		Model B	
	Standardized path weight	*t* value	Standardized path weight	*t* value
PCS → aIPS	0.71	63.5	0.71	63.5
aIPS → vIPS	0.77	18.6	–	–
aIPS → LOC	–	–	0.67	21.8
pIPS → PCS	0.44	17.6	0.44	17.6
pIPS → aIPS	0.21	19.1	0.21	19.1
pIPS → vIPS	1.01	27.1	–	–
pIPS → LOC	–	–	0.89	26.0
vIPS → PCS	−0.05	−2.1	−0.05	−2.1
vIPS → LOC	0.99	55.3	−0.88	−18.9
LOC → PCS	0.29	13.0	0.29	13.0
LOC → vIPS	−1.14	−18.9	1.01	55.3

4. Discussion

The present study shows that a distributed network of cerebral cortical regions is selectively active during HS perception, compared to HT perception. Since performance was statistically similar across conditions, these regions can be considered to play a specific role in processing of haptic shape. The network is bilateral even though haptic exploration was performed using only the right hand. The active regions were in the PCS, three distinct parts of the IPS (aIPS, pIPS and vIPS) and the LOC. Of these areas, the LOC and IPS regions can be considered as multisensory shape-selective regions, since they showed shape-selectivity in both visual and haptic modalities in most subjects, while the PCS was bimodally shape-selective in only one of six subjects and hence is best considered as a mainly unisensory (haptic) area. This is consistent with the identification of the PCS as corresponding to Brodmann's area 2, based on direct comparison of anatomical landmarks and cytoarchitectonics (Grefkes, Geyer, Schormann, Roland, & Zilles, 2001). Brodmann's area 2 is traditionally regarded as part of primary somatosensory cortex. The IPS foci (in posterior parietal cortex) and the LOC (in occipitotemporal cortex), can be considered to be at higher hierarchical levels than the PCS, although currently there is inadequate information to place the IPS regions and the LOC relative to one another in a somatosensory processing hierarchy. It should be noted that the occurrence of bisensory shape-selectivity was not perfectly consistent across subjects. Our study used central visual presentations but right-lateralized haptic presentations; hence, the issue of multisensory processing regions bears further examination under fully equivalent conditions across modalities. It would also be of interest to compare

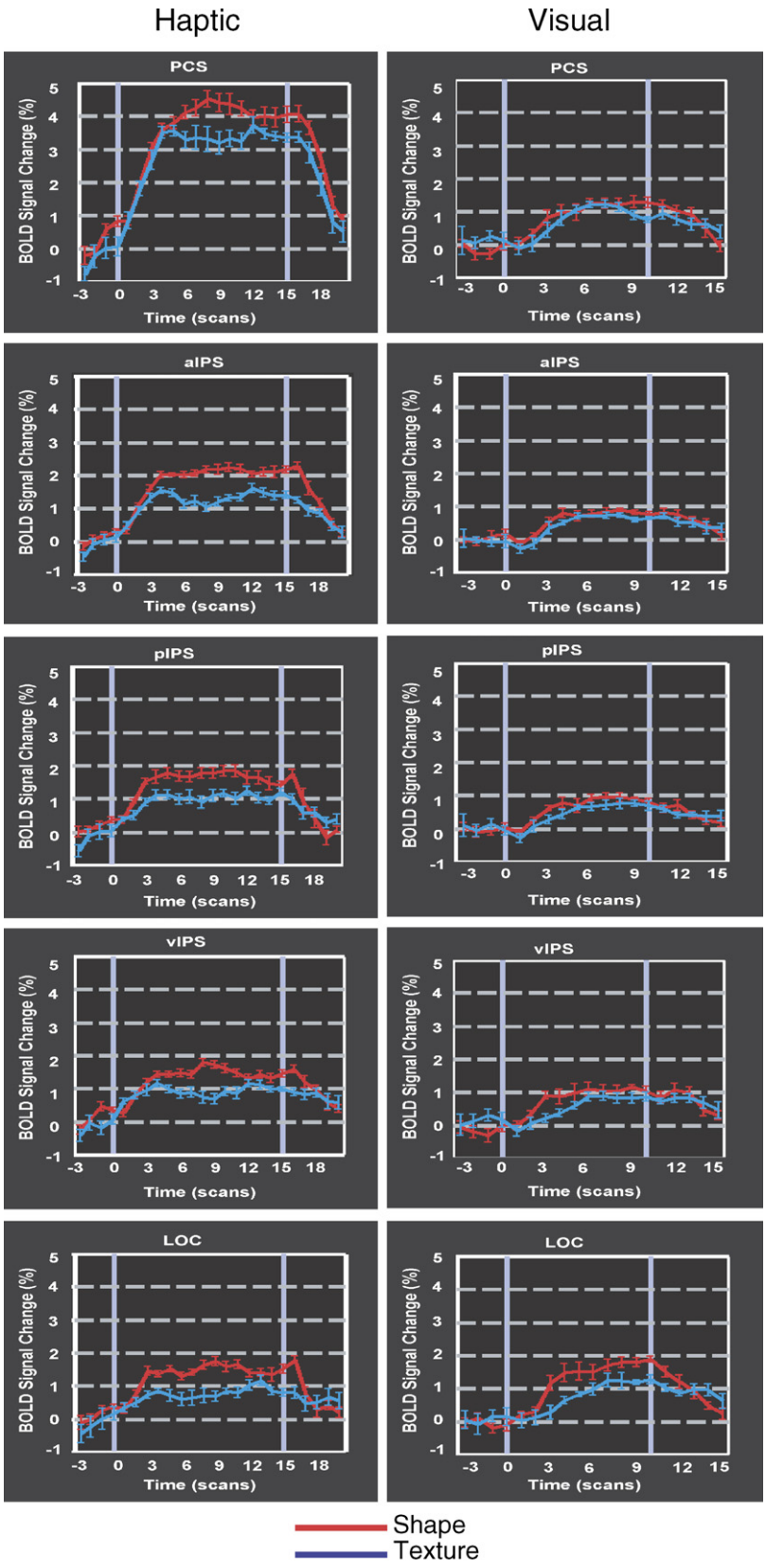

Fig. 2. Time-courses of the BOLD signal, averaged across blocks and runs, for subject 5. Left panel: haptic conditions; right panel: visual conditions.

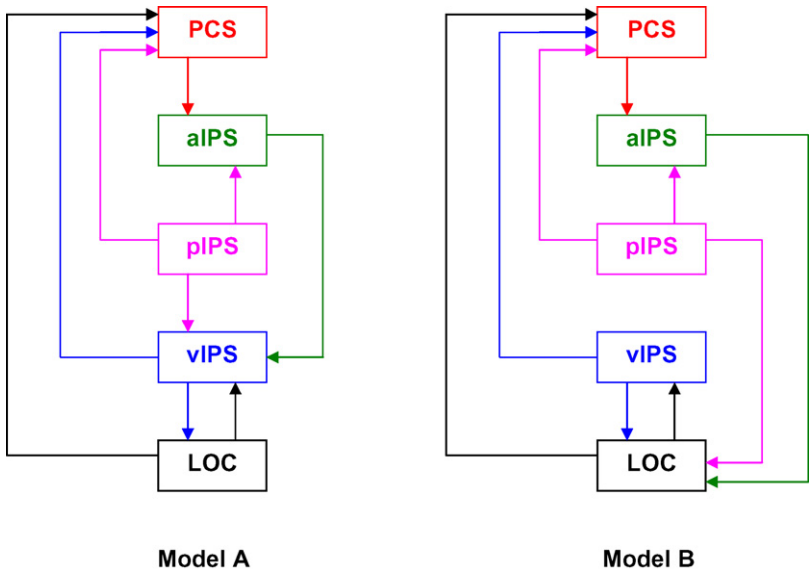

Fig. 3. Top-ranked structural equation models for left-hemisphere haptically shape-selective ROIs.

the effective connectivity of multisensory regions during haptic and visual perception using lateralized stimulus presentations in both modalities.

As outlined below, some prior studies have identified one or more of these regions as involved in haptic or bisensory perception of shape, but the full range of haptically shape-selective areas has not been described previously. Activity during haptic shape perception has been found previously, at or near the foci of the present study, in the PCS (Bodegård et al., 2000; Bodegård, Geyer, Grefkes, Zilles, & Roland, 2001; Servos, Lederman, Wilson, & Gati, 2001), aIPS (Roland, O'Sullivan, & Kawashima, 1998; Zhang et al., 2004), pIPS (Jäncke, Kleinschmidt, Mirzazade, Shah, & Freund, 2001; Stoeckel et al., 2004; Van de Winckel et al., 2005) and LOC (Amedi et al., 2001; Amedi et al., 2002; James et al., 2002; Reed et al., 2004; Stoeckel et al., 2003; Zhang et al., 2004).

Multisensory (haptic and visual) shape-selective activity has been described previously in the LOC (Amedi et al., 2001; Amedi et al., 2002; James et al., 2002; Zhang et al., 2004), aIPS (Grefkes, Weiss, Zilles, & Fink, 2002) and in a caudal region of the IPS (Saito, Okada, Morita, Yonekura, & Sadato, 2003) situated between the pIPS and vIPS loci of the present study. The LOC has attracted particular attention for its multisensory shape-selectivity, owing to its location in the ventral visual pathway that is specialized for form perception. It has been considered the site of a common neural representation for visual and haptic shape. This idea is supported by cross-modal priming effects in fMRI studies (Amedi et al., 2001; James et al., 2002) and by the report of tactile agnosia accompanying visual agnosia in a patient with a lesion that presumably damaged the LOC, but with otherwise intact somatic sensation (Feinberg, Rothi, & Heilman, 1986). However, the LOC is apparently not active during auditory object identification, suggesting a specific role in object geometry (Amedi et al., 2002). It should be noted that the LOC is actually a complex of areas, of which only a part appears to be involved in bisensory (visual and tactile) perception. This part has been termed LOtv by some investigators (Amedi et al., 2002). While the LOC clearly seems to be a major locus of visual and haptic shape processing, cortex of the IPS appears to be involved in a variety of tasks (Culham & Kanwisher, 2001). For instance, the aIPS region appears to have a multisensory role, not only in shape perception, but also during contralateral attention in both vision and touch (Macaluso, Frith, & Driver, 2002), mental rotation of visual (Cohen et al., 1996) and tactile stimuli (Prather et al., 2004), and motion processing of visual, auditory or tactile stimuli (Bremmer et al., 2001). Thus, the nature of the contribution of areas in the IPS to shape processing remain to be worked out.

The winning structural equation models in the present work not only fit the empirical data well, but also have path weights that are each significant. The most significant path in the models is that from PCS to aIPS, which is also the most likely a priori structural connection, given that the PCS corresponds to Brodmann's area 2 (Grefkes et al., 2001), which is known to project to posterior parietal cortex in monkeys (Jones, Coulter, & Hendry, 1978). This finding makes it likely that the aIPS is at a lower hierarchical level than the pIPS, vIPS and LOC foci of the present study. It is apparent in the models that there are both bottom-up (e.g. PCS to aIPS) and top-down (e.g. LOC, vIPS and pIPS to PCS) paths. Thus, there does not appear to be a simple resolution to the issue alluded to in the Introduction, viz. bottom-up versus top-down recruitment of visual and multisensory areas. Rather, the situation is probably much more complex, reflecting an interplay of bidirectional, and possibly even lateral connections, which is in keeping with other multisensory research (e.g., Schroeder et al., 2003).

It must be recognized that the exploratory SEM approach has some limitations, the principal one being the exponential growth in the number of possible models as the number of ROIs increases. This severely limits the number of ROIs for which connectivity can be modelled within an acceptable time frame: at present, testing and ranking all possible models for

five ROIs takes a few days, and hence the present investigation was restricted to five ROIs. This meant that we could only investigate effective connectivity within one hemisphere. We chose the left hemisphere because haptic exploration was performed with the right hand, from which somatosensory inputs initially project to the left hemisphere. The restriction to five ROIs also did not allow us to include ROIs in frontal cortex, which would have been desirable given the known role of prefrontal cortex in mediating visual imagery (Mechelli et al., 2004). The trade-off for accepting the limitation on ROI number is the ability to explore all possible models for the ROIs selected, compared to the standard approach which, although not limited by the number of ROIs, typically investigates only a few models. Despite its limitations, the present study does offer the insight that connectivity between unisensory and multisensory areas is clearly bidirectional, making it likely that both top-down and bottom-up processing is involved in haptic shape perception. The models presented here should be considered candidates for confirmatory analysis in future imaging studies, with extension to frontal cortical areas and transcallosal interactions. Such studies, complemented by neurophysiological and neuroanatomical studies, can be expected to lead to a better understanding of the connections between unisensory and multisensory areas and in turn to clarify the neural mechanisms mediating cross-modal recruitment of visual cortex during normal tactile perception.

Acknowledgement

This work was supported by NIH grants R01EY012440 to KS and R01EB002009 to XH.

References

Amedi, A., Jacobson, G., Hendler, T., Malach, R., & Zohary, E. (2002). Convergence of visual and tactile shape processing in the human lateral occipital complex. *Cerebral Cortex*, *12*, 1202–1212.

Amedi, A., Malach, R., Hendler, T., Peled, S., & Zohary, E. (2001). Visuo-haptic object-related activation in the ventral visual pathway. *Nature Neuroscience*, *4*, 324–330.

Blake, R., Sobel, K. V., & James, T. W. (2004). Neural synergy between kinetic vision and touch. *Psychological Science*, *15*, 397–402.

Bodegård, A., Geyer, S., Grefkes, C., Zilles, K., & Roland, P. E. (2001). Hierarchical processing of tactile shape in the human brain. *Neuron*, *31*, 317–328.

Bodegård, A., Ledberg, A., Geyer, S., Naito, E., Zilles, K., & Roland, P. E. (2000). Object shape differences reflected by somatosensory cortical activation in human. *Journal of Neuroscience*, *20*(RC51), 1–5.

Boecker, H., Khorram-Sefat, D., Kleinschmidt, A., Merboldt, K.-D., Hänicke, W., Requardt, M., et al. (1995). High-resolution functional magnetic resonance imaging of cortical activation during tactile exploration. *Human Brain Mapping*, *3*, 236–244.

Bremmer, F., Schlack, A., Shah, N. J., Zafiris, O., Kubischik, M., Hoffmann, K., et al. (2001). Polymodal motion processing in posterior parietal and premotor cortex: a human fMRI study strongly implies equivalencies between humans and monkeys. *Neuron*, *29*, 287–296.

Brodatz, P. (1966). *Textures. A photographic album for artists and designers*. Mineola, NY: Dover Publications, Inc.

Büchel, C., & Friston, K. (2001). Extracting brain connectivity. In P. Jezzard, P. M. Matthews, & S. M. Smith (Eds.), *Functional MRI. An introduction to methods* (pp. 295–308). Oxford, UK: Oxford University Press.

Calhoun, V. D., Adali, T., Pearlson, G. D., & Pekar, J. J. (2001). Spatial and temporal independent component analysis of functional MRI data containing a pair of task-related waveforms. *Human Brain Mapping*, *13*, 43–53.

Cohen, M. S., Kosslyn, S. M., Breiter, H. C., DiGirolamo, G. J., Thompson, W. L., Anderson, A. K., et al. (1996). Changes in the cortical activity during mental rotation, a mapping study using functional MRI. *Brain*, *119*, 89–100.

Culham, J. C., & Kanwisher, N. (2001). Neuroimaging of cognitive functions in human parietal cortex. *Current Opinion in Neurobiology*, *11*, 157–163.

Feinberg, T. E., Rothi, L. J., & Heilman, K. M. (1986). Multimodal agnosia after unilateral left hemisphere lesion. *Neurology*, *36*, 864–867.

Genovese, C. R., Lazar, N. A., & Nichols, T. (2002). Thresholding of statistical maps in functional neuroimaging using the false discovery rate. *NeuroImage*, *15*, 870–878.

Golay, X., Kollias, S., Stoll, G., Meier, D., Valavanis, A., & Boesiger, P. (1998). A new correlation-based fuzzy logic clustering algorithm for fMRI. *Magnetic Resonance Medicine*, *40*, 249–260.

Grant, A. C., Zangaladze, A., Thiagarajah, M. C., & Sathian, K. (1999). Tactile perception in developmental dyslexia: A psychophysical study using gratings. *Neuropsychologia*, *37*, 1201–1211.

Grefkes, C., Geyer, S., Schormann, T., Roland, P., & Zilles, K. (2001). Human somatosensory area 2: Observer-independent cytoarchitectonic mapping, interindividual variability, and population map. *NeuroImage*, *14*, 617–631.

Grefkes, C., Weiss, P. H., Zilles, K., & Fink, G. R. (2002). Crossmodal processing of object features in human anterior intraparietal cortex: An fMRI study implies equivalencies between humans and monkeys. *Neuron*, *35*, 173–184.

Hagen, M. C., Franzen, O., McGlone, F., Essick, G., Dancer, C., & Pardo, J. V. (2002). Tactile motion activates the human middle temporal/V5 (MT/V5) complex. *European Journal of Neuroscience*, *16*, 957–964.

Hu, L., & Bentler, P. M. (1999). Cutoff criteria for fit indexes in covariance structure analysis: Conventional criteria versus new alternatives. *Structural Equation Modeling*, *6*, 1–55.

James, T. W., Humphrey, G. K., Gati, J. S., Servos, P., Menon, R. S., & Goodale, M. A. (2002). Haptic study of three-dimensional objects activates extrastriate visual areas. *Neuropsychologia*, *40*, 1706–1714.

Jäncke, L., Kleinschmidt, A., Mirzazade, S., Shah, N. J., & Freund, H. J. (2001). The role of the inferior parietal cortex in linking the tactile perception and manual construction of object shapes. *Cerebral Cortex*, *11*, 114–121.

Jones, E. G., Coulter, J. D., & Hendry, S. H. C. (1978). Intracortical connectivity of architectonic fields in the somatic sensory, motor and parietal cortex of monkeys. *Journal of Comparative Neurology*, *181*, 291–348.

Kline, R. B. (1998). *Principles and practice of structural equation modeling*. New York, NY: Guilford Press.

Macaluso, E., Frith, C. D., & Driver, J. (2002). Directing attention to locations and to sensory modalities: Multiple levels of selective processing revealed with PET. *Cerebral Cortex*, *12*, 357–368.

Malach, R., Reppas, J. B., Benson, R. R., Kwong, K. K., Jiang, H., Kennedy, W. A., et al. (1995). Object-related activity revealed by functional magnetic resonance imaging in human occipital cortex. *Proceeding of the National Academy of Sciences of the USA*, *92*, 8135–8139.

Mechelli, A., Price, C. J., Friston, K. J., & Ishai, A. (2004). Where bottom-up meets top-down: Neuronal interactions during perception and imagery. *Cerebral Cortex*, *14*, 1256–1265.

McIntosh, A. R., & Gonzalez-Lima, F. (1994). Structural equation modeling and its application to network analysis in functional brain imaging. *Human Brain Mapping*, *2*, 2–22.

McKeown, M. J., Makeig, S., Brown, G. G., Jung, T. P., Kindermann, S. S., Bell, A. J., et al. (1998). Analysis of fMRI data by blind separation into independent spatial components. *Human Brain Mapping*, *6*, 160–188.

Ngan, S. C., & Hu, X. (1999). Analysis of functional magnetic resonance imaging data using self-organizing mapping with spatial connectivity. *Magnetic Resonance Medicine*, *41*, 939–946.

Prather, S. C., Votaw, J. R., & Sathian, K. (2004). Task-specific recruitment of dorsal and ventral visual areas during tactile perception. *Neuropsychologia*, *42*, 1079–1087.

Raczkowski, D., Kalat, J. W., & Nebes, R. (1974). Reliability and validity of some handedness questionnaire items. *Neuropsychologia*, *12*, 43–47.

Reed, C. L., Shoham, S., & Halgren, E. (2004). Neural substrates of tactile object recognition: An fMRI study. *Human Brain Mapping*, *21*, 236–246.

Roland, P. E., O'Sullivan, B., & Kawashima, R. (1998). Shape and roughness activate different somatosensory areas in the human brain. *Proceedings of the National Academy of Sciences of the USA*, *95*, 3295–3300.

Saito, D. N., Okada, T., Morita, Y., Yonekura, Y., & Sadato, N. (2003). Tactile-visual cross-modal shape matching: A functional MRI study. *Cognitive Brain Research*, *17*, 14–25.

Sathian, K., & Zangaladze, A. (2001). Feeling with the mind's eye: The role of visual imagery in tactile perception. *Optometry and Vision Science*, *78*, 276–281.

Sathian, K., Cascio, C., Rice, D., Morris, M., Dancer, C., & McGlone, F. (2003). Is tactile temporal processing impaired in developmental dyslexia? Cognitive Neuroscience Society Abstracts, 192.

Sathian, K., Prather, S. C., & Zhang, M. (2004). Visual cortical involvement in normal tactile perception. In G. Calvert, C. Spence, & B. Stein (Eds.), *The Handbook of multisensory processes* (pp. 703–709). Cambridge, MA: MIT Press.

Sathian, K., Zangaladze, A., Hoffman, J. M., & Grafton, S. T. (1997). Feeling with the mind's eye. *NeuroReport*, *8*, 3877–3881.

Schroeder, C. E., Smiley, J., Fu, K. G., McGinnis, T., O'Connell, M. N., & Hackett, T. A. (2003). Anatomical mechanisms and functional implications of multisensory convergence in early cortical processing. *International Journal of Psychophysiology*, *50*, 5–17.

Sergent, J., Ohta, S., & MacDonald, B. (1992). Functional neuroanatomy of face and object processing. A positron emission tomography study. *Brain*, *115*, 15–36.

Servos, P., Lederman, S., Wilson, D., & Gati, J. (2001). fMRI-derived cortical maps for haptic shape, texture and hardness. *Cognitive Brain Research*, *12*, 307–313.

Stoeckel, M. C., Weder, B., Binkofski, F., Buccino, G., Shah, N. J., & Seitz, R. J. (2003). A fronto-parietal circuit for tactile object discrimination: An event-related fMRI study. *NeuroImage*, *19*, 1103–1114.

Stoeckel, M. C., Weder, B., Binkofski, F., Choi, H. J., Amunts, K., Pieperhoff, P., et al. (2004). Left and right superior parietal lobule in tactile object discrimination. *European Journal of Neuroscience*, *19*, 1067–1072.

Stoesz, M., Zhang, M., Weisser, V. D., Prather, S. C., Mao, H., & Sathian, K. (2003). Neural networks active during tactile form perception: common and differential activity during macrospatial and microspatial tasks. *International Journal of Psychophysiology*, *50*, 41–49.

Talairach, J., & Tournoux, P. (1988). *Co-planar stereotaxic atlas of the brain.* New York: Thieme Medical Publishers.

Ullman, J. B. (1996). Structural equation modeling. In B. G. Tabachnick & L. S. Fidell (Eds.), *Using multivariate statistics* (3rd ed., pp. 709–819). New York, NY: Harper Collins College.

Van de Winckel, A., Sunaert, S., Wenderoth, N., Peeters, R., Van Hecke, P., Feys, H., et al. (2005). Passive somatosensory discrimination tasks in healthy volunteers: Differential networks involved in familiar versus unfamiliar shape and length discrimination. *NeuroImage*, *26*, 441–453.

Zangaladze, A., Epstein, C. M., Grafton, S. T., & Sathian, K. (1999). Involvement of visual cortex in tactile discrimination of orientation. *Nature*, *401*, 587–590.

Zhang, M., Weisser, V. D., Stilla, R., Prather, S. C., & Sathian, K. (2004). Multisensory cortical processing of object shape and its relation to mental imagery. *Cognitive, Affective and Behavioral Neuroscience*, *4*, 251–259.

Zhuang, J., LaConte, S., Peltier, S., Zhang, K., & Hu, X. (2005). Connectivity exploration with structural equation modeling: An fMRI study of bimanual motor coordination. *NeuroImage*, *25*, 462–470.